portional to the squares of metal-ligand overlap integrals. We have urged, many times, both empirically and theoretically, that the AOM *as used* in ligand-field analysis is *not* a molecular orbital scheme and does not suffer the whole range of deficiencies normally associated with semiempirical and approximate MO models applied to transition-metal systems. We argue, therefore, for a realignment of our prejudices based on well-founded ligand-field theory rather than on more common but inappropriate molecular orbital theory.

**Acknowledgment.** We record our appreciation of useful discussions with Dr. R. G. Woolley.

**Registry No.** $[Cu(bpy)_2I]^+I^-$, 15679-48-8; $[Cu(phen)_2H_2O]^{2+}(NO_3)^-_2$, 57572-96-0; Cu(tet-b)($o$-$SC_6H_4CO_2$), 92471-16-4.

Contribution from the School of Chemical Sciences, University of Illinois, Urbana, Illinois 61801

# Dynamics of Spin-State Interconversion and Cooperativity for Ferric Spin-Crossover Complexes in the Solid State. 1. The Unperturbed Fast Spin-Flipping $N_4O_2$ Complex $[Fe(SalAPA)_2]ClO_4$

WAYNE D. FEDERER[1] and DAVID N. HENDRICKSON*

*Received January 13, 1984*

Samples of the ferric spin-crossover complex $[Fe(SalAPA)_2]ClO_4$, where SalAPA is the monoanionic Schiff base derived from salicylaldehyde and *N*-(3-aminopropyl)aziridine, prepared by two different methods, are shown to have different properties. In the more crystalline samples, $[Fe(SalAPA)_2]ClO_4$ is one of the relatively rare $N_4O_2$ ferric spin-crossover complexes that flip spins between the low-spin and high-spin states at a rate faster than the $^{57}Fe$ Mössbauer time scale. On the other hand, the less crystalline sample of $[Fe(SalAPA)_2]ClO_4$ shows two quadrupole-split doublets in the Mössbauer spectrum from ~150 to 205 K. Differences are also seen in the magnetic susceptibility and EPR characteristics for these two types of samples, in spite of the fact that both sample types have the same chemical analyses and IR spectra and similar (lines are sharper in more crystalline samples) powder X-ray diffraction patterns. It is concluded that the less crystalline sample type has a greater concentration of defect structure than the crystalline samples that give one (average) quadrupole-split doublet. The increased defect structure results in a certain fraction of the ferric complexes either persisting totally in the high-spin state across the temperature range or more slowly interconverting between low- and high-spin states. Both types of samples of $[Fe(SalAPA)_2]ClO_4$ are found to flip spins faster than a sample of the related $N_4O_2$ complex, $[Fe(SalAEA)_2]ClO_4$, which contains the monoanionic ligand derived from salicylaldehyde and *N*-(2-aminoethyl)aziridine. The factors that lead to certain $N_4O_2$ ferric spin-crossover complexes flipping spins faster by at least 1 order of magnitude than other $N_4O_2$ complexes are discussed.

## Introduction

Spin-crossover behavior has been observed for complexes of $Mn^{3+}$ ($d^4$),[2] $Mn^{2+}$ ($d^5$),[3] $Co^{3+}$ ($d^6$),[4] $Co^{2+}$ ($d^7$),[5] and $Ni^{2+}$ ($d^8$),[6] for inorganic solids containing $Mn^{3+}$,[7] $Fe^{2+}$,[8] or $Co^{3+}$,[9] and for cluster compounds of niobium.[10] The results for ferrous spin-crossover complexes, which have received by far the greatest attention, are summarized in a comprehensive and recent review by Gütlich.[11] Spin-crossover ferric complexes, also quite prominent in the literature since the initial work by Cambi et al.[12] on the tris(dithiocarbamates), were last reviewed by Martin and White;[13] a more current account by Sinn is forthcoming.[14]

In the last few years attention has been directed to understanding the kinetics and mechanisms of the spin-crossover transformation. A given complex interconverts between low-spin and high-spin electronic states in what amounts to an intramolecular electron-transfer reaction. In the *solution state* it appears that there is a dynamic equilibrium present with a Boltzmann distribution of spin-crossover complexes in low-spin ground and high-spin excited states, as indicated by variable-temperature magnetic susceptibility data (Evans technique). Relaxation techniques have been used to measure spin-crossover interconversion rates for complexes in *solution*.[15-24] Buhks et al.[25] have applied the theory of radiationless nonadiabatic multiphonon processes in order to estimate the rate of spin-state interconversion of complexes in *solution*.

Most investigations of the physical properties of spin-crossover complexes have been conducted exclusively on samples in the *solid state*. Spin-crossover transformations come

(1) 3M Fellowship, 1979-1980. Owens-Corning Fellowship, 1980-1981. Present address: Magnetic Audio/Video Products Division, 3M, St. Paul, MN 55144.
(2) Sim, P. G.; Sinn, E. *J. Am. Chem. Soc.* **1981**, *103*, 241.
(3) Ammeter, J. H.; Zoller, L.; Bachmann, J.; Baltzer, E.; Gamp, E.; Bucher, R.; Deiss, E. *Helv. Chim. Acta* **1981**, *64*, 1063.
(4) Klaui, W. *J. Chem. Soc., Chem. Commun.* **1979**, 700.
(5) Barefield, E. K.; Busch, D. H.; Nelson, S. M. *Q. Rev., Chem. Soc.* **1968**, *22*, 457.
(6) Sacconi, L. *Pure Appl. Chem.* **1971**, *27*, 161.
(7) Haneda, S.; Noriaki, K.; Yamaguchi, Y.; Watanabe, H. *J. Phys. Soc. Jpn.* **1977**, *42*, 31.
(8) Eibschütz, M.; Lines, M. E. *Phys. Rev. Lett.* **1977**, *39*, 726.
(9) Ramasesha, S.; Ramakrishnan, T. V.; Rao, C. N. R. *J. Phys. C* **1979**, *12*, 1307.
(10) Imoto, H.; Simon, A. *Inorg. Chem.* **1982**, *21*, 308.
(11) Gütlich, P. *Struct. Bonding (Berlin)* **1981**, *44*, 83.
(12) (a) Cambi, L.; Cagnasso, A. *Atti. Accad. Naz. Lincei, Cl. Sci. Fis., Mat. Nat., Rend.* **1931**, *13*, 809. (b) Cambi, L.; Szego, L. *Ber. Dtsch. Chem. Ges.* **1931**, *64*, 2591.
(13) Martin, R. H.; White, A. H. *Transition Met. Chem. (N.Y.)* **1968**, *4*, 113.
(14) Sinn, E., private communication.
(15) Binstead, R. A.; Beattie, J. K.; Dewey, T. G.; Turner, D. H. *J. Am. Chem. Soc.* **1980**, *102*, 6442.
(16) Binstead, R. A.; Beattie, J. K.; Dose, E. V.; Tweedle, M. F.; Wilson, L. J. *J. Am. Chem. Soc.* **1978**, *100*, 5609.
(17) Beattie, J. K.; Binstead, R. A.; West, R. J. *J. Am. Chem. Soc.* **1978**, *100*, 3044.
(18) Reeder, K. A.; Dose, E. V.; Wilson, L. J. *Inorg. Chem.* **1978**, *17*, 1071.
(19) Petty, R. H.; Dose, E. V.; Tweedle, M. F.; Wilson, L. J. *Inorg. Chem.* **1978**, *17*, 1064.
(20) Dose, E. V.; Hoselton, M. A.; Sutin, N.; Tweedle, M. F.; Wilson, L. J. *J. Am. Chem. Soc.* **1978**, *100*, 1141.
(21) Simmons, M. G.; Wilson, L. J. *Inorg. Chem.* **1977**, *16*, 126.
(22) Dose, E. V.; Murphy, K. M. M.; Wilson, L. J. *Inorg. Chem.* **1976**, *15*, 2622.
(23) Hoselton, M. A.; Drago, R. S.; Wilson, L. J.; Sutin, N. *J. Am. Chem. Soc.* **1976**, *98*, 6967.
(24) Beattie, J. K.; Sutin, N.; Turner, D. H.; Flynn, G. W. *J. Am. Chem. Soc.* **1973**, *95*, 2052.
(25) Buhks, E.; Navon, G.; Bixon, M.; Jortner, J. *J. Am. Chem. Soc.* **1980**, *102*, 2918.

0020-1669/84/1323-3861$01.50/0 

in a variety of types, as judged by variable-temperature magnetic susceptibility data. Some are essentially discontinuous; within a few degrees the sample changes between the high-spin excited and low-spin ground states. Heat capacity measurements[26] and observations of thermal hysteresis[27] clearly indicate that these discontinuous transformations are in fact first-order phase transitions. In the case of these discontinuous transformations, the cooperativity probably results from significant long-range electron–phonon coupling. Sorai and Seki[26] explained their heat capacity results on $Fe(phen)_2(NCS)_2$ and $Fe(phen)_2(NCSe)_2$ in terms of domains, that is, appreciably sized, homogeneous regions of minority spin-state phase present in the majority phase. More recently Haddad et al.[28-30] used the nucleation and growth mechanism of phase transitions in solids[31] to account for the degree of sharpness in the transition as well as incomplete transitions and the sensitivity of spin-crossover systems to solvation and sample preparation.

Gradual spin-crossover transformations in the solid state are by far more common than are the discontinuous type. Pronounced hysteresis has been seen for at least one gradual $Fe^{2+}$ complex,[32] suggesting the presence of a first-order phase transition for this compound. In general, however, little is known of the nature and mechanism of gradual transformations. In a very recent study of one $Fe^{2+}$ complex undergoing a gradual transformation, König et al.[33] carefully analyzed variable-temperature Mössbauer and powder X-ray diffraction data. They concluded that the two spin isomers form a solid solution within the same lattice, a crystallographic phase change is not involved, and consequently the transformation develops over a wide range of temperature. They concluded that domain formation is essentially absent in this complex. Until recently the tris complexes of dithio-,[34] diseleno-,[35] or monothiocarbamates[36] with $Fe^{3+}$ were the only ferric compounds that flip spin at a rate *faster* than detectable by the $^{57}Fe$ Mössbauer technique ($> \sim 10^7$ $s^{-1}$), as manifested by the presence of a single, population-weighted average Mössbauer quadrupole doublet at all temperatures.[36] For the dithio- and diselenocarbamate complexes, *upper* limits for the spin-flipping rates have been established[34] by EPR data as less than $\sim 10^{10}$ $s^{-1}$. It was thought that these $Fe^{3+}$ dithiocarbamate and related complexes were unique in the realm of ferric spin-crossover complexes. All others interconvert at a rate *slower* than can be detected by the Mössbauer technique (less than $\sim 10^6$ $s^{-1}$). The increased covalency and spin–orbit interactions present in these $FeS_6$ complexes were thought to be the origin of the relatively fast interconversion rates. However, Maeda et al.[37-39] very recently reported three $Fe(N_4O_2)$ complexes that are interconverting *faster* than detected by the Mössbauer technique. Federer et al.[28,40] also reported one such $N_4O_2$ ferric spin-crossover complex that was flipping spin at a fast rate at room temperature.

In this and the following paper new experimental results (via $^{57}Fe$-enriched samples) are presented for $[Fe(SalAPA)_2]ClO_4$, where SalAPA is the monoanionic Schiff base derived from salicylaldehyde and *N*-(3-aminopropyl)aziridine. Results are presented in this paper for "unperturbed" microcrystalline samples of $[Fe(SalAPA)_2]ClO_4$ (identified as FeP) and in the following paper for "perturbed" samples of FeP obtained by solvation or grinding of FeP.

## Experimental Section

**Physical Measurements.** It must first be emphasized that, unless specified otherwise, all physical measurements were conducted on samples in the same physical state as described in the section on sample preparation. Samples were *not* pulverized to eliminate effects of incomplete or nonrandom distributions of polycrystalline orientations. The presence of any such effects will be noted where it is considered pertinent to the interpretation of results.

**Elemental Analyses.** Analyses for C, H, N, Cl, Fe, and Co were performed by the School of Chemical Sciences Microanalytical Service. The violent nature of the metal perchlorate decomposition sometimes caused experimental difficulties, in particular for the chlorine determinations, which tended to give results higher than the true values.

**Infrared Spectra.** IR spectra of 13-mm KBr pellets (~2 mg of sample/100 mg of KBr) were recorded over the range 4000–250 $cm^{-1}$ on a Perkin-Elmer Model 599B spectrophotometer. Wavenumbers were calibrated with a polystyrene film.

**NMR Spectra.** Proton NMR spectra were run on a 90-MHz Varian EM-390 spectrometer with $Me_4Si$ as calibrant.

**Magnetic Susceptibilities.** Variable-temperature (4–307 K) magnetic susceptibilities were determined on a Princeton Applied Research Model 150A parallel-field vibrating-sample magnetometer. Measurements were conducted with applied fields of 13.75 kG and a calibrated GaAs diode for temperature control and measurement, in conjunction with a $CuSO_4 \cdot 5H_2O$ calibrant. The details of operation and calibration of this system have been previously described.[41] Effective magnetic moments, $\mu_{eff}$/Fe, were calculated after suitable corrections for diamagnetism.[42]

**X-ray Powder Diffraction Measurements.** Interplanar spacings were determined by the Debye–Scherrer method using Cu K$\alpha$ radiation and a 114.6-mm camera with 0.7-mm aperture. The effective camera diameter was measured with a sodium chloride calibrant. Lengthy exposure times (~22 h) of the Kodak NS-392T film were necessary to combat the very significant X-ray absorption by the iron and cobalt samples, which were packed into 0.7-mm glass capillaries. The errors reported are estimates based on the distribution of the centers of gravity that were calculated for each of the broad diffraction arcs.

**Mössbauer Spectra.** The zero-field Mössbauer spectra for FeE and sample **X2** of FeP were acquired on Prof. P. Debrunner's system that has been described elsewhere.[43] All other Mössbauer results were obtained on a recently completed constant-acceleration spectrometer. Considerable detail is available about the construction of this new spectrometer.[44] The presence of a 60-kG superconducting magnet in the Janis Research Co. Model 12-CNDT cryostat necessitated a vertical-drive configuration. Because the temperature of the cooled $^{57}Co$ source (40–30 mCi during data collection) varies with absorber temperature in such a vertical-drive spectrometer, the experimental

(26) Sorai, M.; Seki, S. *J. Phys. Chem. Solids* **1974**, *35*, 555.
(27) (a) König, E.; Ritter, G. *Solid State Commun.* **1976**, *18*, 279. (b) König, E.; Ritter, G.; Irler, W. *Chem. Phys. Lett.* **1979**, *66*, 336. (c) König, E.; Ritter, G.; Kulshreshtha, S. K.; Nelson, S. M. *Inorg. Chem.* **1982**, *21*, 3022. (d) König, E.; Ritter, G.; Irler, W.; Goodwin, H. A. *J. Am. Chem. Soc.* **1980**, *102*, 4681. (e) König, E.; Ritter, G.; Irler, W.; Nelson, S. M. *Inorg. Chim. Acta* **1979**, *37*, 169. (f) Sorai, M.; Ensling, J.; Hasselback, K. M.; Gutlich, P. *Chem. Phys.* **1977**, *20*, 197.
(28) Haddad, M. S.; Federer, W. D.; Lynch, M. W.; Hendrickson, D. N. "Coordination Chemistry"; Laurent, J. P., Ed.; Pergamon Press: Oxford, 1981; Vol. 21, p 75.
(29) (a) Haddad, M. S.; Lynch, M. W.; Federer, W. D.; Hendrickson, D. N. *Inorg. Chem.* **1981**, *20*, 123. (b) *Ibid.* **1981**, *20*, 131.
(30) Haddad, M. S.; Federer, W. D.; Lynch, M. W.; Hendrickson, D. N. *J. Am. Chem. Soc.* **1980**, *102*, 1468.
(31) Rao, C. N. R.; Rao, K. J. "Phase Transitions in Solids"; McGraw-Hill: New York, 1978.
(32) Ritter, G.; König, E.; Irler, W.; Goodwin, H. A. *Inorg. Chem.* 1978, *17*, 224.
(33) König, E.; Ritter, G.; Kulshreshtha, S. K.; Nelson, S. M. *J. Am. Chem. Soc.* **1983**, *105*, 1924.
(34) Hall, G. R.; Hendrickson, D. N. *Inorg. Chem.* **1976**, *15*, 607 and references cited therein.
(35) DeFilipo, D.; Depalano, P.; Diaz, A.; Steffe, S.; Trogu, E. F. *J. Chem. Soc., Dalton Trans.* **1977**, 1566.
(36) Kunze, K. R.; Perry, D. L.; Wilson, L. J. *Inorg. Chem.* **1977**, *16*, 594.
(37) Maeda, Y.; Tsutsumi, N.; Takashima, Y. *Chem. Phys. Lett.* **1982**, 88, 248.
(38) Maeda, Y.; Ohshio, H.; Takashima, Y. *Chem. Lett.* **1982**, 943.
(39) Ohshio, H.; Maeda, Y.; Takashima, Y. *Inorg. Chem.* **1983**, *22*, 2684.
(40) Federer, W. D.; Haddad, M. S.; Lynch, M. W.; Hendrickson, D. N. "Abstracts of Papers", 179th National Meeting of the American Chemical Society, Houston, TX, March 1980; American Chemical Society: Washington, D.C., 1980; NUCL 74.
(41) Duggan, D. M.; Barefield, E. K.; Hendrickson, D. N. *Inorg. Chem.* **1973**, *12*, 985.
(42) Figgis, B. N.; Lewis, J. "Modern Coordination Chemistry"; Lewis, J., Wilkins, R. G., Eds.; Interscience: New York, 1960; p 403.
(43) Münck, E.; Debrunner, P. G.; Tsibris, J. C. M.; Gunsalus, I. C. *Biochemistry* **1972**, *11*, 855.
(44) Federer, W. D. Ph.D. Thesis, University of Illinois, 1984.

velocity scales of spectra recorded at different temperatures must be corrected by different amounts in order for the reported center-shift parameter to be expressed conventionally as velocity relative to iron metal for both *source and absorber at 298 K*. For this purpose, a standard curve was prepared from (a) variable-temperature center shifts measured for iron foil under the present experimental conditions and (b) the suitably converted variable-temperature shifts for iron, as reported by Preston, Hanna, and Heberle,[45] which were obtained by using a $^{57}Co$ source maintained at 77 K. We estimate the *absolute* precision of our reported velocities relative to iron as no better than ±0.03 mm/s, due to variability in the flow rate and pressure of cryogenic gas in the sample region. However, for a given variable-temperature run the flow was kept rather constant, so the relative precision of the center-shift determination within a series of spectra is considerably better. The velocity scales shown on all plotted spectra have *not* been corrected whatsoever; thus, the center shift cannot be correctly visualized. Such information can only be obtained from tables of the corrected parameters, expressed relative to iron metal and $^{57}Co$ source at 298 K. Either a calibrated copper–constantan thermocouple (100–190 K) or a Yellow Springs No. 44003A precision thermistor (190–311 K), also mounted in the sample cell holder, is used for temperature measurement (estimated absolute precision ±3 K; relative precision ±0.5 K).

Mössbauer spectra were analyzed with several computer programs. Lorentzian fits involving one or two quadrupole doublets, each having components of equal areas, were obtained with MOSBFIT,[46] a slightly modified version of a program previously described. Magnetic Mössbauer spectra were simulated with the versatile spin Hamiltonian program FERSPEC,[47] which was obtained from Prof. P. Debrunner.

**EPR Spectra.** X-band (9.11-GHz) spectra were obtained over the range 105–338 K with a Varian E-9 spectrometer equipped with a gas-flow cavity insert and a Varian V-4540 temperature controller. Temperatures were determined before and after each spectrum with a calibrated copper–constantan thermocouple; the precision is comparable to that of the Mössbauer temperature measurements. Temperatures of 77 K were achieved with a quartz immersion Dewar. Liquid-helium spectra (4 K at 9.39 GHz) were recorded on a Bruker ER-200D spectrometer equipped with an Oxford cavity insert. The relative precision of our reported $g$ values is estimated to be ±0.003; the poorer absolute precision (±0.01) is limited by uncertainties in the magnetic field calibration.

**Sample Preparation.** Except where indicated otherwise, all chemicals, including solvents, were of reagent grade and were used without further purification. *Caution! The complex perchlorate salts reported here are all heat sensitive, igniting explosively if subjected to sudden temperature increases. They are also mildly shock sensitive, as evidenced by one occasion where a sample of FeP exploded after ~30 min of hand grinding by mortar and pestle, sending a small brown mushroom cloud into the air. Suitable personal safety precautions must be taken at all times!*

**Reagents.** The metal perchlorate salts were purchased from G. Frederick Smith. Iron metal of natural isotopic composition was in the form of a gray electrolytic powder supplied by Fisher. A similar though slightly more reactive material containing 95.27% iron-57 isotope (atomic wt = 57.002) was furnished by Spire Corp. and stored in a vacuum desiccator prior to use.

*N*-(2-aminoethyl)aziridine (AEA) was obtained as a gift from Dow Chemical. It was either used as received or distilled from a mixture of itself and the trimer and tetramer of aziridine. The fraction taken was that boiling over the range 69–73 °C (100 mm). Purity was checked by gas chromatography as described by Root.[48]

*N*-(3-aminopropyl)aziridine (APA) was synthesized from *N*-(2-cyanoethyl)aziridine that was obtained from Polysciences, Inc., or Dow Chemical. The $LiAlH_4$ reduction of the nitrile was achieved by a fivefold scaleup of the preparation reported by Salerni and Clark.[49] The reactants were kept under argon in a three-necked flask fitted with an overhead stirrer. It is especially important to wash the thick, granular white solids formed during quenching of the reaction mixture with copious quantities (~3500 mL) of ether in order to extract as much product as possible. A yield of 26.3 g (25%) of the colorless liquid (bp 67–70 °C (20–21 mm)) was obtained after three successive vacuum distillations. Purity was checked by proton NMR (–0.98 (t, 2 H), –1.30 (s, 2 H), –1.50 (m, 4 H), –2.10 (t, 2 H), –2.60 ppm (t, 2 H)) and infrared (amine vibrations 3370, 3295, 1600 $cm^{-1}$; $-CH_2-$ vibrations 3058, 2980, 2925, 2840, 1483, 1448 $cm^{-1}$; no evidence of bands assignable to secondary amine impurities) spectroscopies of the neat liquid.

Salicylaldehyde was obtained from Aldrich or Eastman and was distilled at atmospheric pressure when found to be significantly discolored.

**$[Fe(SalAEA)_2]ClO_4$, FeE.** For the present work, a sample of FeE that was synthesized during an earlier study was reexamined.[50] The yellow Schiff base solution was prepared by mixing 1.22 g (0.0100 mol) of salicylaldehyde and 0.86 g (0.010 mol) of AEA in 100 mL of absolute methanol in a 250-mL round-bottomed flask. Crystals of ferrous perchlorate hexahydrate (1.81 g, 0.005 00 mol) were introduced to the stirring solution. The reaction mixture immediately assumed an intense purple color, and a small quantity of the purple product was deposited onto the walls of the flask. After 5 min, 1 mL of 4 M sodium hydroxide (0.004 mol) was added. After about 5 h of stirring at room temperature, the volume was reduced to about 15 mL on a rotary evaporator. Filtration and a wash with cold water and then several portions of diethyl ether afforded 2.1 g of a fluffy powder.

For recrystallization, the compound was dissolved in a minimum volume of dichloromethane and the hot solution was gravity filtered. Boiling cyclohexane was added gradually until the volume ratio of the two solvents was 4:1 (dichloromethane/cyclohexane). The solution was allowed to evaporate undisturbed until the volume was under 20 mL. The purple crystals formed were clumped together and appeared irregular and possibly twinned. A yield of 1.96 g (73.4%) of the complex was isolated after two such purifications. The product was dried for 17 h at 50 °C in vacuo.

**$[Co(SalAEA)_2]ClO_4$, CoE.** The perchlorate salt of CoE was prepared by metathesis of a sample of $[Co(SalAEA)_2]Cl\cdot 2H_2O$ that was generously provided by Dr. C. A. Root. The complex perchlorate precipitated as a finely divided, pale brown powder upon mixing of 1.01 g (0.002 00 mol) of the chloride and 5.62 g (0.0400 mol) of $NaClO_4\cdot H_2O$ in 60 mL of methanol. Filtration 1 day later of the solution that had been stored in a freezer gave 0.68 g of the crude product, which dissolved quantitatively in the 400 mL of 3:1 methanol/dichloromethane used for recrystallization. The 0.45 g of brown microcrystalline product was isolated by slow evaporation to near dryness (~35 mL), filtration, washes with methanol, and then ether, and finally drying overnight in a vacuum desiccator.

**$Fe_{0.50}Co_{0.50}E$.** Equal 100-mg aliquots of FeE and CoE were dissolved in a mixture of 125 mL of dichloromethane and 10 mL of nitromethane. The purple solution was filtered and boiled down to 10 mL with no precipitation occurring. Another 20 mL of dichloromethane and 50 mL of cyclohexane were then introduced. Beautiful purple microcrystals were suspended in the now very pale brown solution after ~2 h. The 150 mg of $Fe_{0.50}Co_{0.50}E$ was isolated by filtration, washed with cyclohexane and then ether, and dried over $P_2O_5$ in vacuo.

**"Unperturbed" Samples of $[Fe(SalAPA)_2]ClO_4$, FeP. U1.** Hydrated ferrous chloride was freshly prepared as follows. Isotopically enriched iron-57 metal powder (27.2 mg, 0.477 mmol) was dissolved in ~8 mL of concentrated hydrochloric acid with the aid of heating of the 50-mL pear-shaped flask for ~5 min in an oil bath maintained at 163–175 °C. The excess HCl was effectively removed at room temperature by rotary evaporation to dryness. The pale yellow solids were promptly redissolved in ~5 mL of methanol, giving an orange solution.

The ligand solution, consisting of salicylaldehyde (114 mg, 0.933 mmol) and a slight molar excess of APA (104 mg, 1.04 mmol) dissolved in 25 mL of methanol, was combined with 10 mL of a methanolic solution containing 2.50 g (17.8 mmol) of $NaClO_4\cdot H_2O$. To the resulting mixture was introduced the ferrous chloride solution as several small aliquots. The dark purple microcrystals (134 mg, 0.237 mol, 51%) that formed within 60 s were isolated promptly by filtration, washed with ether, and dried over Drierite for 48 h in vacuo.

(45) Preston, R. S.; Hanna, S. S.; Heberle, J. *Phys. Rev.* **1962**, *128*, 2207.
(46) Chrisman, B. L.; Tumolillo, T. A. *Comput. Phys. Commun.* **1971**, *2*, 322.
(47) Munck, E.; Groves, J. L.; Tumolillo, T. A.; Debrunner, P. G. *Comput. Phys. Commun.* **1973**, *5*, 252.
(48) Root, C. A.; Rising, B. A.; VanDerveer, M. C.; Hellmuth, C. F. *Inorg. Chem.* **1972**, *11*, 1489. AEA is now commercially available from Polysciences, Inc.
(49) Salerni, O. L.; Clark, R. N. *J. Med. Chem.* **1966**, *9*, 778.
(50) Federer, W. D. M.S. Thesis, Bucknell University, Lewisburg, PA, 1977.

**U2.** An approximately fourfold scaleup of the preparation described for **U1** was conducted with naturally abundant iron metal (100.0 mg, 1.791 mmol). The only other apparent difference was a somewhat reduced yield (371 mg, 0.660 mmol, 36%).

**U3.** This reaction was conducted with reagent quantities scaled up by a factor of 8 compared to those used to prepare **U1**. However, the solvent volumes were increased by only a factor of 6. The yield of **U3** was 881 mg (1.57 mmol, 43%).

The unperturbed samples **U1**, **U2**, and **U3** consist of clustered needles of lengths <0.1 mm. Microscopic examination also reveals an occasional colorless cubic impurity crystal (NaCl). The deviations of microanalytical results from the calculated values, notably for sample **U2**, may be explained in terms of a relatively minor NaCl contaminant.

**Samples of FeP Prepared from Ferrous Perchlorate. X1.** This sample was prepared in a fashion very similar to that already described for FeE. A purple solution and precipitate resulted from the addition of 0.91 g (0.0025 mol) of $Fe(ClO_4)_2 \cdot 6H_2O$ to a mixture containing 0.61 g (0.0050 mol) of salicylaldehyde and 0.50 g (0.0050 mol) of APA in 50 mL of absolute ethanol. A 0.5-mL portion (0.002 mol) of 4 M NaOH was then introduced. Several hours later, 1.07 g (76%) of a purple powder was isolated from the reaction mixture. Recrystallization required ~300 mL of dichloromethane for dissolution and then 75 mL of cyclohexane to induce crystallization upon evaporation of the chloroalkane. Some reddish brown residue was left behind during the initial purification. The solvent mixture was evaporated down to ~30 mL prior to filtration. After three recrystallizations the product (0.75 g, 54%) was triturated in ether and vacuum desiccated for 16 h at 50 °C.

**X2.** This sample was obtained by the same procedure as **X1**, except that methanol rather than ethanol was chosen for the reaction mixture.

## Results and Discussion

**Compound Preparation and Structure.** Two new bis(tridentate) complexes of iron(III) with $N_4O_2$ coordination cores have been prepared with

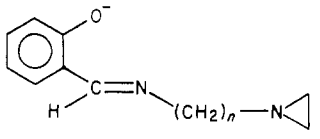

SalAEA, $n = 2$
SalAPA, $n = 3$

In this and the following paper in the series the complexes $[Fe(SalAEA)_2]ClO_4$ and $[Fe(SalAPA)_2]ClO_4$ will be identified as FeE (E for ethylene) and FeP (P for propylene), respectively. Microcrystalline samples of FeE and FeP were prepared by condensation of the Schiff base components of the ligand in an aerobic alcoholic solution containing either ferrous perchlorate and sodium hydroxide (method 1) or ferrous chloride and a large excess of sodium perchlorate (method 2). Method 2, which is by far the better method, was devised to prepare $^{57}Fe$-enriched samples for detailed Mössbauer work (vide infra). A major practical difference between the two methods of preparation is that the crude powders obtained in method 1 required purification by repeated recrystallizations from dichloromethane/cyclohexane mixtures, whereas method 2 afforded pure microcrystalline solids directly from the mother liquor.

Two samples of FeP, labeled **X1** and **X2**, were prepared by method 1. Three samples of FeP, labeled **U1**, **U2**, and **U3**, were prepared by method 2. The sample **U1** was made from iron metal containing 95.27% $^{57}Fe$. Microanalytical data are given in Table I[51] for all of the above samples and for the one sample of FeE studied, which was prepared by method 1.

The proposed structures for the iron(III) complex cations in the salts FeE and FeP are illustrated in Figure 1. At present it has not been possible to grow suitable crystals for an X-ray structural determination of either of these compounds. However, a crystal structure of an analogue of FeP

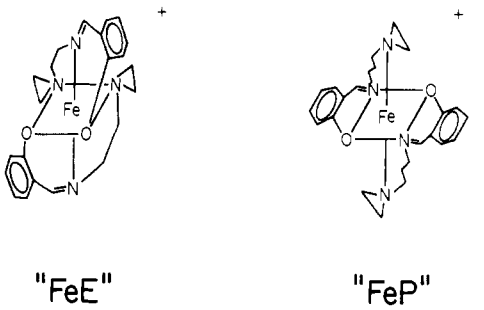


**Figure 1.** Proposed meridional (cis oxygen) structure for the cationic complex "FeE" and centrosymmetric facial (all trans) structure for the cationic complex "FeP".

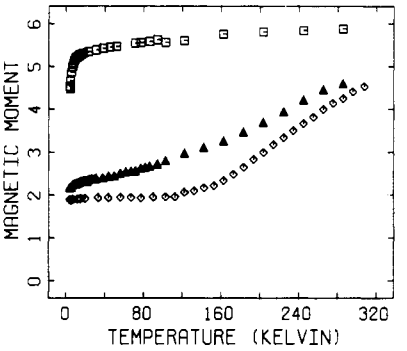


**Figure 2.** Plots of effective magnetic moment per ferric ion, $\mu_{eff}$/Fe, vs. temperature: FeE, □; sample **U1** of FeP, ◇; sample **X2** of FeP, ▲.

where the salicylaldehyde is substituted with a 3-ethoxy substituent has very recently completed; a centrosymmetric cation as pictured in Figure 1 was found.[52] That the iron(III) cations present in FeE and FeP are meridional (cis oxygen donors) and facial (all donors trans) geometric isomers, respectively, may also be inferred from several pieces of indirect evidence. X-ray structures have been reported for several analogues of FeE, where two $N_2O$ tridentate Schiff-base ligands with ethylene linkages between imine and amine nitrogen donors are present.[53-55] Structures are also available[57] for ferric complexes with hexadentate $N_4O_2$ ligands derived from triethylenetetramine. The X-ray crystallographic determinations for these structural analogues of FeE have invariably shown the geometry to be meridional. X-ray powder diffraction data were collected for FeP and FeE; see Table II.[51] There is not a one-to-one correspondence of all reflections for FeE and FeP. This indicates that the two complexes crystallize in different space groups.

**Magnetic Susceptibility.** One sample of FeE and four samples of FeP (**X1**, **X2**, **U1**, **U2**) were examined with the variable-temperature magnetic susceptibility technique. The results are given in Tables III–VII.[51] The variations of the effective magnetic moment for FeE and the **X2** and **U1** samples of FeP are illustrated in Figure 2.

The magnetic data for samples **X1** and **U2** of FeP are not illustrated in Figure 2 because the data for these two samples are very similar to those illustrated for samples **X2** and **U1**, respectively. It is clear from Figure 2 that the two different

(51) Supplementary material.

(52) Abdel-Mawgoud, A.-M. M.; Wilson, S.; Hendrickson, D. N., unpublished results.
(53) Summerton, A. P.; Diamantis, A. A.; Snow, M. R. *Inorg. Chim. Acta* **1978**, *27*, 123.
(54) Sim, P. G.; Sinn, E.; Petty, R. H.; Merrill, C. L.; Wilson, L. J. *Inorg. Chem.* **1981**, *20*, 1213 and references cited therein.
(55) Sinn, E.; Timken, M. D.; Hendrickson, D. N., unpublished results.
(56) Sinn, E.; Sim, G.; Dose, E. V.; Tweedle, M. F.; Wilson, L. J. *J. Am. Chem. Soc.* **1978**, *100*, 3375.
(57) Greenwood, N. N.; Gibb, T. C. "Mössbauer Spectroscopy"; Chapman and Hall: London, 1971; pp 50–53 and references cited therein.

Table IX. Mössbauer Parameters for Sample X2 of FeP (Four-Line Lorentzian Fits)[a]

| T, K | F(HS)[b] | CS, mm/s | QS, mm/s | $\Gamma_{1/2}$(−), mm/s | $\Gamma_{1/2}$(+), mm/s | $\chi^2(11)$[c] |
|---|---|---|---|---|---|---|
| 293 | 0.8 (5) | 0.31 (1) | 1.09 (2) | 0.37 (2) | 0.44 (2) | 0.49 |
| | | 0.5 (4) | 1.4 (8) | 1.1 (6) | 1.1 (6) | |
| 269 | 0.6 (4) | 0.33 (5) | 0.75 (9) | 0.32 (5) | 0.38 (5) | 0.45 |
| | | 0.30 (7) | 1.5 (2) | 0.34 (6) | 0.42 (6) | |
| 248 | 0.6 (2) | 0.38 (2) | 0.99 (4) | 0.38 (3) | 0.37 (2) | 0.97 |
| | | 0.26 (7) | 1.6 (1) | 0.42 (5) | 0.7 (1) | |
| 238 | 0.55 (7) | 0.36 (1) | 0.89 (3) | 0.33 (2) | 0.35 (1) | 0.82 |
| | | 0.28 (2) | 1.83 (3) | 0.34 (2) | 0.35 (2) | |
| 233 | 0.47 (5) | 0.36 (1) | 0.88 (3) | 0.35 (2) | 0.37 (2) | 0.63 |
| | | 0.27 (1) | 2.00 (2) | 0.32 (2) | 0.30 (1) | |
| 227 | 0.41 (2) | 0.383 (8) | 0.85 (2) | 0.30 (1) | 0.31 (1) | 1.06 |
| | | 0.276 (5) | 1.98 (1) | 0.32 (1) | 0.30 (1) | |
| 215 | 0.36 (2) | 0.395 (7) | 0.82 (1) | 0.29 (1) | 0.30 (1) | 1.21 |
| | | 0.278 (4) | 2.00 (1) | 0.32 (1) | 0.30 (1) | |
| 181 | 0.25 (3) | 0.42 (3) | 0.84 (4) | 0.28 (2) | 0.41 (4) | 1.24 |
| | | 0.28 (1) | 2.15 (1) | 0.36 (1) | 0.39 (1) | |
| 149 | 0.15 (1) | 0.45 (2) | 0.73 (5) | 0.22 (3) | 0.30 (3) | 0.60 |
| | | 0.27 (1) | 2.40 (1) | 0.26 (1) | 0.25 (1) | |
| 90 | 0.15 (1) | 0.45 (1) | 0.75 (2) | 0.25 (2) | 0.27 (2) | 0.82 |
| | | 0.278 (2) | 2.452 (2) | 0.229 (2) | 0.207 (2) | |
| ~25 | 0.05 (3) | 0.20 (4)[d] | 0.78 (7) | 0.18 (4) | 0.32 (7) | 0.76 |
| | | 0.056 (1)[d] | 2.406 (2) | 0.177 (2) | 0.159 (2) | |

[a] Parameters obtained with assumption of equal areas for the two component peaks of each quadrupole doublet. Errors in last significant figures are given in parentheses. [b] Area fraction of high-spin (inner) doublet. [c] $\chi$-squared value indicating quality of data and of fit to 11 adjustable parameters, except for 293 K where only 10 parameters were used because the low-spin line widths were set equal. [d] Experimental values, not corrected for deviation of $^{57}$Co source temperature from 298 K.

methods of preparation of FeP give products that show appreciable differences in their susceptibility data. Relative to the data for **U1** and **U2**, there is a "plateau" in the $\mu_{eff}$ vs. temperature data for **X1** and **X2**. It can be seen that not only are there more high-spin molecules at high temperatures for the type **X** samples compared to type **U** samples but also the spin-crossover transformation is not complete for the type **X** samples. That is, below ~80 K there are some high-spin molecules that resist the conversion to the low-spin state even though the thermal energy present is quite small. Method 1 was the earlier of the two methods used to prepare FeP. Sample **X2** was first studied with variable-temperature Mössbauer spectroscopy, and it was our initial excitement about an apparent cross relaxation between high- and low-spin states, as evidenced by line broadening and coalescence in the Mössbauer spectra (see ref 28 and 40), that led to the detailed studies described in this paper. That there is no significant chemical difference between samples of FeP prepared by the two methods is demonstrated by the essentially identical appearances of their infrared spectra and their powder X-ray diffraction patterns. It is our opinion that either the crystallization process is poorer or it is the removal of the $CH_2Cl_2$ solvate from type **X** samples by vacuum desiccation that leads to an increased concentration of defect structure. In fact, sample **X2** was found to diffract rather poorly compared to sample **U1**. As we suggested recently,[28-30] an increased defect structure leads to a more gradual spin-crossover transformation and to plateaus (i.e., residual high-spin molecules) in the $\mu_{eff}$ vs. temperature curves.

Examination of Figure 2 shows that FeE is quite a different material than FeP. At room temperature, FeP contains approximately equal numbers of low- and high-spin complexes, whereas only the high-spin state of FeE is significantly populated. In marked contrast to FeP, the compound FeE exhibits a "high-plateauing" behavior in its $\mu_{eff}$ vs. $T$ plot; even at 20 K there is no more than 20% population of the low-spin state. The rather abrupt drop in $\mu_{eff}$ for FeE below 20 K is likely due to zero-field splitting of the high-spin state. The magnetic susceptibility data alone do not provide unequivocal proof that FeE is a spin-crossover complex. Spectroscopic techniques (vide infra) are necessary to demonstrate the presence of low-spin complexes.

**Mössbauer Spectroscopy.** The zero-field Mössbauer spectra shown in Figure 3 offer the clearest evidence for coexisting low- and high-spin states in FeE. The parameters resultant from fitting these spectra to Lorentzian lines are summarized in Table VIII.[51] The 293 K spectrum exhibits only a broad high-spin ferric doublet with an apparent quadrupole splitting of ~0.7 mm/s. As the temperature of the sample is lowered, a low-spin doublet with a splitting of ~3.0 mm/s grows into the spectrum. This is in agreement with our analysis of the low-spin EPR signal observed for magnetically dilute FeE complexes (vide infra). Perhaps the most important conclusion that can be drawn from Figure 3 is that, at temperatures all the way up to 250 K, molecules of FeE are interconverting between low- and high-spin states slower than $\sim 10^6$ s$^{-1}$.

In a preliminary study of sample **X2** of FeP, Federer et al.[40] concluded that there was evidence for line broadening and coalescence of low- and high-spin Mössbauer signals. It was suggested that, as the sample temperature was increased above liquid-nitrogen temperature, FeP molecules began to interconvert between the low-spin ground-state Kramers doublet and the array of three high-spin Kramers doublets *at a rate that affected the line shape of the Mössbauer signals*. These preliminary data for sample **X2** were of inferior quality. A somewhat improved data set was collected for sample **X2**, and this together with a least-squares fit to two pairs (quadrupole-split doublets) of Lorentzian peaks are illustrated in Figure 4. The fitting parameters are given in Table IX. Two doublets, one for low-spin and the other for high-spin complexes, are clearly visible in the 90–238 K spectra. Over the range of 238–293 K the spectrum collapses inward; there is a pronounced decrease in the low-spin quadrupole splitting (outer doublet) and a slight increase in the high-spin value with increasing temperature. The centroids of the two doublets converge toward the same velocity as the sample temperature is raised. The center shift for Mössbauer lines normally decreases with increasing temperature (above a very low-temperature plateau) by virtue of the second-order Doppler effect.[57] No such trend is followed for the low-spin (outer) doublet in Figure 5. Another anomaly evident in these new data for sample **X2** is the substantial broadening of each Lorentzian line as the temperature is increased. These findings suggest, as was pointed out in our preliminary communica-

Table X. Mössbauer Parameters for Sample U1 of FeP (Two-Line Lorentzian Fits)[a]

| $T$, K | CS, mm/s | QS, mm/s | $\Gamma_{1/2}(-)$, mm/s | $\Gamma_{1/2}(+)$, mm/s | ln $A$[c] | $\chi^2(6)$[e] |
|---|---|---|---|---|---|---|
| 311 | +0.300 (2) | 1.168 (3) | 0.304 (2) | 0.383 (3) | 0.974 (5) | 0.37 |
| 300 | 0.290 (1) | 1.152 (3) | 0.308 (2) | 0.378 (3) | 1.079 (5) | 0.46 |
| 286 | 0.290 (1) | 1.180 (3) | 0.323 (2) | 0.388 (3) | 1.231 (4) | 0.50 |
| 276 | 0.294 (1) | 1.219 (3) | 0.346 (2) | 0.398 (3) | 1.356 (4) | 1.07 |
| 264 | 0.294 (2) | 1.297 (4) | 0.368 (3) | 0.403 (4) | 1.478 (6) | 2.13 |
| 251 | 0.292 (3) | 1.412 (5) | 0.393 (5) | 0.413 (5) | 1.604 (8) | 4.77 |
| 244 | 0.289 (3) | 1.522 (6) | 0.399 (6) | 0.403 (6) | 1.692 (10) | 6.85 |
| 231 | 0.282 (3) | 1.682 (6) | 0.388 (5) | 0.383 (5) | 1.790 (10) | 6.90 |
| 220 | 0.274 (2) | 1.825 (5) | 0.359 (5) | 0.347 (4) | 1.859 (9) | 6.89 |
| 210 | 0.267 (2) | 1.962 (4) | 0.326 (4) | 0.311 (4) | 1.911 (8) | 4.49 |
| 200 | 0.264 (1) | 2.089 (3) | 0.297 (3) | 0.287 (2) | 1.957 (6) | 2.55 |
| 188 | 0.264 (1) | 2.188 (2) | 0.270 (2) | 0.263 (2) | 1.983 (6) | 1.63 |
| 177 | 0.264 (1) | 2.276 (2) | 0.253 (2) | 0.244 (2) | 2.010 (5) | 1.60 |
| 165 | 0.266 (1) | 2.327 (2) | 0.245 (2) | 0.241 (2) | 2.039 (6) | 1.52 |
| 153 | 0.271 (1) | 2.362 (2) | 0.234 (2) | 0.232 (2) | 2.047 (6) | 2.38 |
| 136 | 0.275 (1) | 2.390 (2) | 0.231 (2) | 0.233 (2) | 2.094 (7) | 2.13 |
| 111 | 0.280 (1) | 2.400 (2) | 0.238 (2) | 0.241 (2) | 2.168 (7) | 2.16 |
| 133 | 0.064 (1)[b] | 2.364 (2) | 0.236 (2) | 0.238 (2) | 2.080 (6)[d] | 5.42 |
| 121 | 0.059 (1)[b] | 2.379 (2) | 0.237 (2) | 0.241 (2) | 2.126 (6)[d] | 6.96 |
| 110 | 0.055 (1)[b] | 2.383 (2) | 0.241 (2) | 0.247 (2) | 2.168 (6)[d] | 4.98 |
| 98 | 0.053 (1)[b] | 2.386 (2) | 0.246 (2) | 0.251 (2) | 2.210 (7)[d] | 6.11 |
| 86 | 0.050 (1)[b] | 2.388 (2) | 0.249 (2) | 0.256 (2) | 2.249 (7)[d] | 5.45 |
| 76 | 0.048 (1)[b] | 2.391 (2) | 0.256 (2) | 0.261 (2) | 2.290 (7)[d] | 5.03 |
| 61 | 0.046 (1)[b] | 2.393 (2) | 0.258 (2) | 0.265 (2) | 2.327 (7)[d] | 3.93 |
| 46 | 0.046 (1)[b] | 2.390 (3) | 0.265 (2) | 0.271 (3) | 2.373 (7)[d] | 4.13 |
| 34 | 0.045 (1)[b] | 2.395 (3) | 0.273 (3) | 0.281 (3) | 2.416 (7)[d] | 4.12 |
| 24 | 0.046 (1)[b] | 2.397 (3) | 0.277 (2) | 0.285 (3) | 2.432 (7)[d] | 3.69 |
| 13 | 0.047 (1)[b] | 2.394 (3) | 0.291 (3) | 0.303 (3) | 2.436 (7)[d] | 3.42 |

[a] Parameters obtained with assumption of equal areas for the two component peaks of a single quadrupole doublet. Errors in last significant figures are given in parentheses. [b] These experimental shifts, obtained for spectra recorded with liquid helium as cryogen, have not been corrected to be relative to iron metal calibrant. [c] Natural logarithm of background-normalized area of total fitted spectrum (sum of counts in all channels divided by base line counts). [d] These values of ln $A$ for liquid-helium run have been arbitrarily decreased by 0.764, in order to make the ln $A$ vs. $T$ curve continuous. The correction is necessitated by instrumental factors (involving the counting electronics and possibly also the velocity drive). [e] $\chi$-squared value indicating quality of data and of fit to six adjustable parameters.

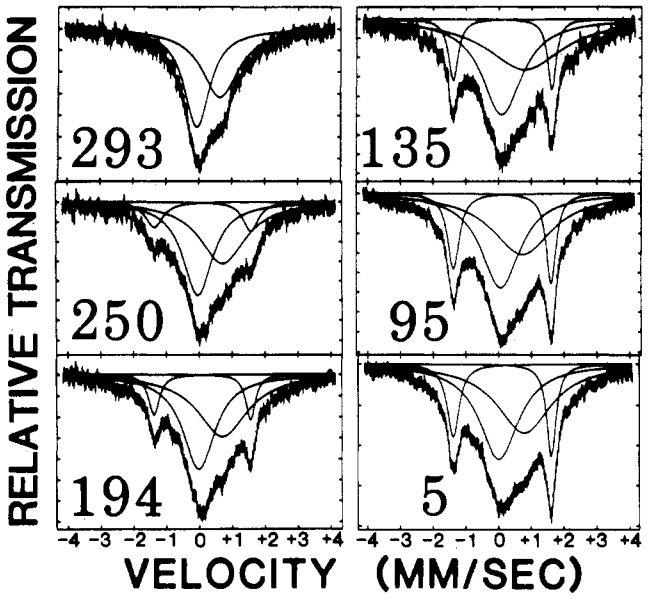


**Figure 3.** Variable-temperature Mössbauer spectra for FeE in zero magnetic field. The spectra are fit to four Lorentzians. Labels correspond to temperatures in Kelvin.

tions,[28,40] that the high-spin and low-spin resonances are actually coalescing into a single population-weighted average quadrupole doublet at ~240 K. As it turns out, this explanation for the appearance of the spectra illustrated in Figure 4 did *not* stand the test of time.

The signal-to-noise ratio of the spectra shown in Figure 4 was still not totally satisfying. As a consequence, we decided to prepare a 95% $^{57}$Fe-enriched sample of FeP instead of carrying out a least-squares fit of the spectra in Figure 4 to a two-site relaxation model to obtain relaxation rate data. A new small-scale preparation of FeP (method 2, type U samples) was devised to prepare FeP starting with 95% $^{57}$Fe iron metal. This second method gave microcrystalline FeP straightaway without recrystallization. The appearance of the Mössbauer spectra for FeP prepared by this second synthetic method is even more amazing! A representative sampling of the large number of zero-field spectra recorded for the $^{57}$Fe-enriched sample U1 is displayed in Figure 5. Two-line (one doublet) Lorentzian fits and the corresponding parameters are given in Figure 6 and Table X, respectively. The appearance of a single average quadrupole doublet over the entire temperature range indicates that the high-spin and low-spin complexes are interconverting at a rate considerably faster than $\sim 10^7$ s$^{-1}$. The complex FeP joins the $N_4O_2$ complexes [Fe(acen)(dpp)]$BPh_4$, [Fe(acen)(pic)$_2$]$BPh_4$, and [Fe(bzpa)$_2$]$PF_6$ reported very recently by Maeda et al.[37-39] and the solvated complex FeP·$CH_2Cl_2$ (see following paper) as the only "fast" spin-crossover complexes that do not have very "soft" covalently bonded ligand donor atoms (i.e., S or Se atoms).

The pronounced temperature dependence of the quadrupole splitting and center shift for sample U1 of FeP is plotted in Figure 6. The low-temperature limit of $\Delta E_Q$ = 2.4 mm/s corresponds to the quadrupole splitting for the low-spin FeP. As indicated by the EPR results (vide infra), the ground state for low-spin FeP is a single Kramers doublet of largely $d_{xy}$ orbital character and the other two low-spin Kramers doublets are at too high an energy to be populated at 300 K. Consequently, little temperature dependence is expected for the quadrupole splitting of low-spin FeP complexes. A plot of the observed splitting for FeP vs. the high-spin fraction (as obtained by interpolation of the values calculated from the susceptibility data of Table III) is quite linear over the temperature range of 276–177 K (correlation coefficient $R_{corr}$ = 0.996). The anomalous variable-temperature behavior of the Mössbauer center shift for sample U1 of FeP (see Figure 6)

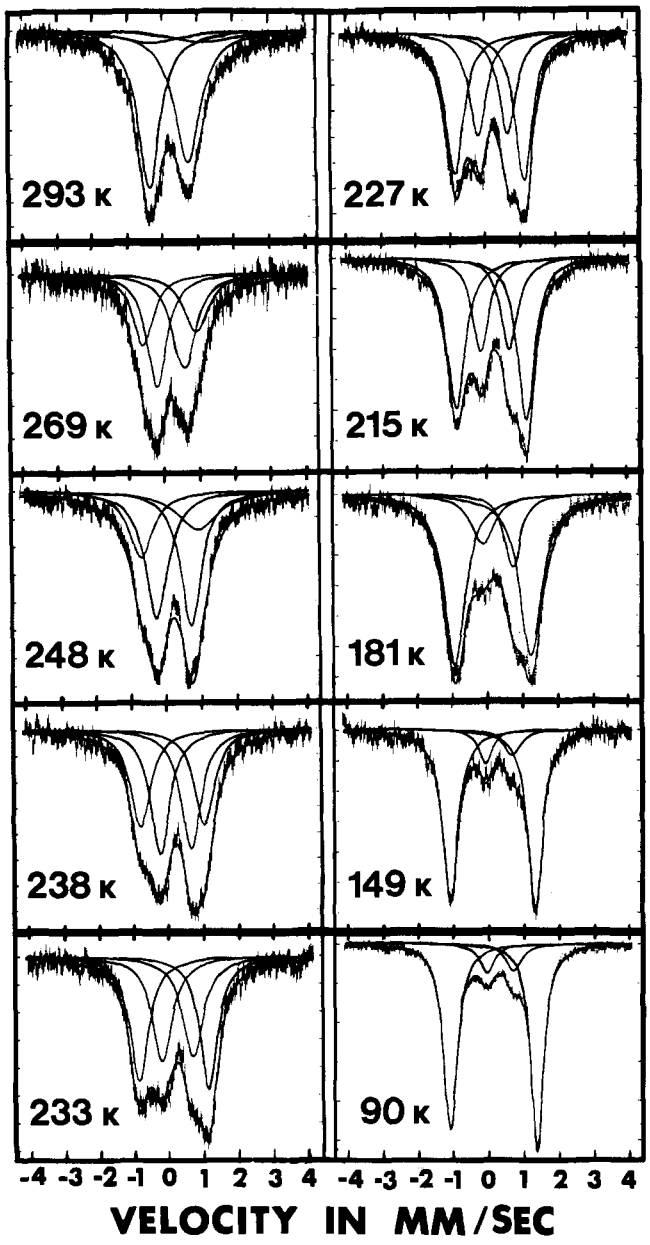


**Figure 4.** Variable-temperature Mössbauer spectra for sample X2 of FeP. The spectra are fit to four Lorentzians.

is also consistent with the conclusion that the single quadrupole doublet is a population-weighted average of signals for low- and high-spin complexes.

Plots of line half-width of the Lorentzian lines vs. temperature for the two components of the doublet in the FeP spectra reveal distinct maxima in the vicinity of 245 K. This observation is interpreted as a clue that the low-spin $\rightleftharpoons$ high-spin interconversion rate may be only barely faster than can be discerned by Mössbauer spectroscopy.

The extremely favorable counting statistics observed for sample U1 allow us to examine critically the line shapes of our spectra. As can be seen in Figure 6 the lower velocity component of the 231 and 251 K spectra has a decidedly non-Lorentzian appearance, which renders our fits rather unsatisfactory. A shoulder is visible on the lower velocity component. Although the appearance of these two spectra suggests that coalescence of the low-spin and high-spin resonances is *almost* (but not totally) complete, it could be argued reasonably that there are actually two strongly overlapping quadrupole doublets present over this more limited temperature range that encompasses the line width maxima. Other explanations can be advanced for the presence of more than one doublet at a given temperature. First, the shouldering (inner)

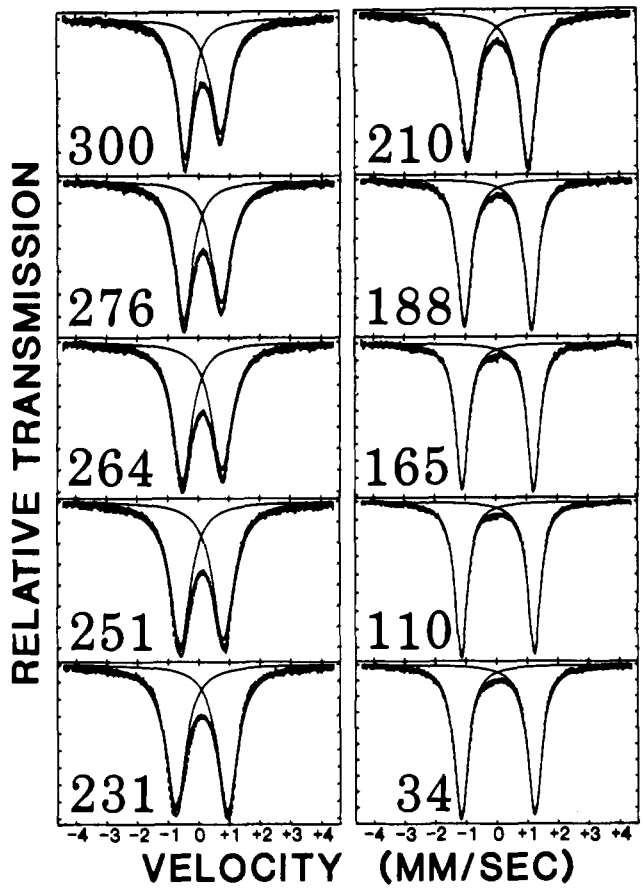


**Figure 5.** Variable-temperature Mössbauer spectra and two-line Lorentzian fits for $^{57}$Fe-enriched sample U1 of FeP (absorber concentration 0.93 mg of $^{57}$Fe/cm$^2$).

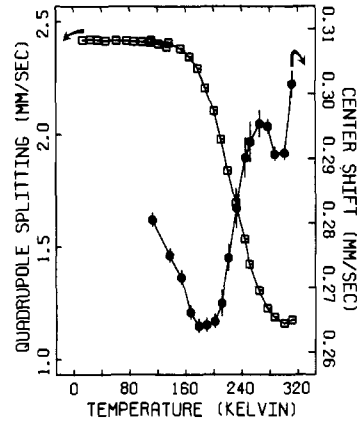


**Figure 6.** Plot of Mössbauer quadrupole splitting (□) and center shift (●) vs. temperature for sample U1 of FeP. Center shift data for temperatures below 111 K are omitted because they have not been corrected to remove the contribution from the $^{57}$Co/Rh source. Error bars have been omitted from the quadrupole-splitting plot because the error bars are smaller than the symbols.

doublet could be associated with high-spin FeP complexes that are located near a defect structure, that is, cracks, fissures, dislocations, etc., or at the surface of the crystallites. These "residual" high-spin FeP complexes would not be involved in the spin-crossover interconversion due to the strains in their local environments. Second, the shouldering doublet could be due to a number of low- and high-spin complexes that are interconverting at a lower rate at a given temperature than are the complexes that give rise to the outer doublet.

If there are high-spin FeP complexes located at defect sites, it should be possible to apply an external magnetic field and see a magnetic Mössbauer pattern characteristics of a high-spin species unless the high-spin complexes are relaxing too fast.

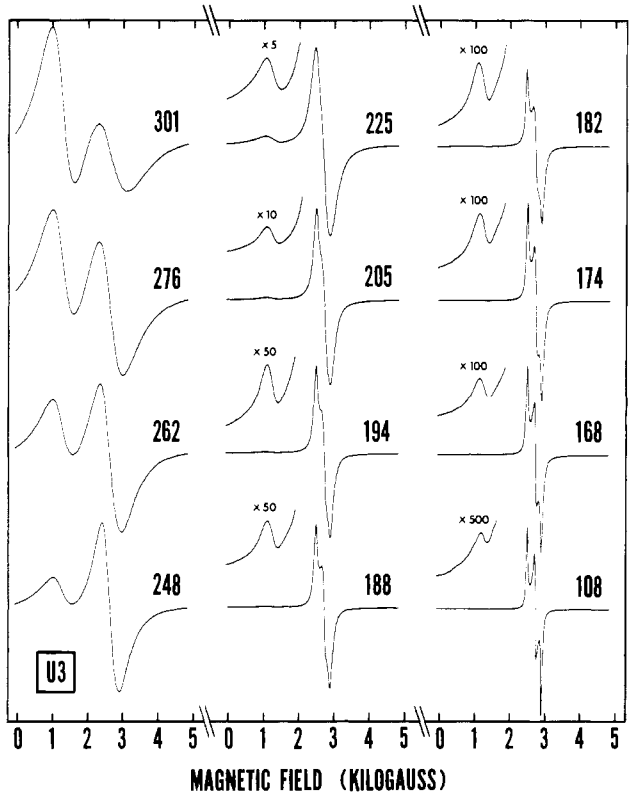


**Figure 7.** Variable-temperature X-band (9.11-GHz) EPR spectra for sample U3 of FeP. Labels correspond to temperatures in Kelvin.

A longitudinal field of 58 kG was applied to sample **U1**, and Mössbauer spectra were recorded at intervals over the range 34–313 K. At several temperatures spectra were recorded over larger velocity ranges of ±10 mm/s. There is no evidence at any temperature of a magnetic pattern with the large internal field characteristic of a high-spin ferric complex. The observed magnetic Mössbauer spectrum taken at 34 K was simulated with a simple model suitable for diamagnetic compounds using the FERSPEC computer program.[47] Experimental and simulated spectra are available in the supplementary material. The simulation of this 34 K spectrum shows that the sign of the electric field gradient in the low-spin ground state is negative. A negative electric field gradient is consistent with the $d_{xy}$ Kramers doublet ground state indicated by the EPR results (vide infra).

**Electron Paramagnetic Resonance.** Samples of FeE and FeP were examined with EPR spectroscopy, both as solids and in frozen solutions. Figure 7 shows a progression of EPR spectra recorded for sample **U3** of FeP at various temperatures. A very similar series of spectra was obtained for the $^{57}$Fe-enriched sample **U1**; however, the small sample size led to a situation where there was interference from a signal arising from a small amount of microwave cavity contamination. Each spectrum in Figure 7 exhibits two resonances, a broad isotropic ($g \simeq 4.3$) high-spin signal and a rhombic low-spin pattern in the $g \simeq 2$ region. The relative intensities for low-spin and high-spin species vary with temperature in a manner roughly paralleling the results from the magnetic susceptibility measurements. The observation of two distinct EPR features assignable to low-spin and high-spin species at every temperatures shows that the spin-flipping rate for the type **U** samples of FeP is considerably slower than the X-band frequency of $\sim 10^{10}$ s$^{-1}$.

Representative frozen-solution EPR spectra for FeE and FeP are displayed in Figure 8. These two perchlorate salts have their greatest solubilities ($\sim 10^{-2}$ M) in polar aprotic solvents such as acetone, acetonitrile, dimethylformamide, dimethyl sulfoxide, nitromethane, or dichloromethane. FeE

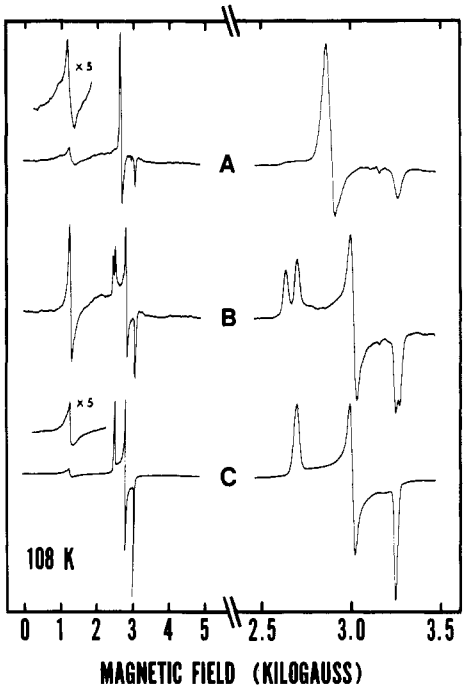


**Figure 8.** X-band (9.11 GHz) EPR spectra for frozen solutions at 108 K: (A) FeE in 2:3 (v/v) $CH_2Cl_2$/toluene; (B) sample **U3** of FeP in 2:3 (v/v) $CH_2Cl_2$/toluene; (C) sample **G1** (for origin of this sample see next paper) of FeP in 1:1 (v/v) methanol/glycerol.

is generally more soluble than FeP. The complexes are also sparingly soluble in methanol and ethanol but are insoluble in nonpolar solvents such as benzene, cyclohexane, diethyl ether, hexanes, or toluene. As can be seen in Figure 8, dilute ($\leq 10^{-3}$ M) dichloromethane/toluene solutions of both complexes give spectra (trace A for FeE and trace B for FeP) that show sizable high-spin and low-spin contributions at 108 K. However, for FeP there are *two* different rhombic low-spin signals. One of these two rhombic signals ($g$ = 2.349, 2.109, 1.951) is rather similar to that found for a solid sample of the solvate FeP·$CH_2Cl_2$, a compound characterized in the following paper. The other rhombic signal ($g$ = 2.409, 2.109, 1.939) is virtually identical with the more anisotropic signal observed for sample **X2** of FeP. The same two rhombic EPR signals are also observed for FeP in a frozen solution of absolute ethanol. However, only one low-spin rhombic EPR signal is found for frozen solutions of FeP in acetone/toluene and methanol/glycerol (trace C) mixtures.

A closer look at the low-spin EPR $g$ values is appropriate, for they provide information concerning the energetics and the orbital constitution of the three low-spin Kramers doublets. The set of three $g$ values for each low-spin EPR signal was least-squares fit with a computer program that directly calculates effective $g$ values by diagonalizing 6 × 6 matrices resultant from using the following ligand field Hamiltonian for the $^2T_{2g}$ state of low-spin $d^5$ ion in a magnetic field (hole formalism):

$$\mathcal{H} = \zeta \hat{l}\cdot\hat{s} - \delta(\hat{l}_z^2 - \tfrac{2}{3}) - \frac{\epsilon}{2}(\hat{l}_+^2 + \hat{l}_-^2) + (\hat{l} + 2\hat{s})\beta\cdot\hat{H}_i$$

$$i = x, y, z$$

In this equation $\zeta$ is the one-electron spin–orbit coupling constant, $\delta$ and $\epsilon$ are the axial and rhombic distortion parameters, and $\hat{H}_i$ is the applied magnetic field oriented along a molecular axis $x$, $y$, or $z$. In this approach, the observed $g$ values for the $\Gamma_1(^2T_{2g})$ state are analyzed to give the energies ($E_1$, $E_2$, $E_3$) as well as the constitution (in terms of $A$, $B$, $C$ coefficients) of the three $^2T_{2g}$ Kramers doublets. Previous analyses have employed equations derived from perturbation theory.[29,30]

Experimental $g$ values for the complexes in this paper and the results of a least-squares fitting of these $g$ values are given in Table XII.[51] Data are also included for the previously reported[29,30] complex $[Fe(3\text{-}OMe\text{-}SalEen)_2]PF_6$, where the $N_2O$ tridentate ligand results from the condensation of 3-methoxysalicylaldehyde and *N*-ethylethylenediamine. This complex undergoes discontinuous (i.e., sudden) spin-crossover transformation at ~159 K; that is, within ~2 K the whole sample changes from high spin to low spin. This material has a nearly axial **g** tensor with $g$ values of 2.220, 2.187, and 1.946. The complex $[Fe(3\text{-}OMe\text{-}SalEen)_2]PF_6$ is typical of other $N_4O_2$ spin-crossover ferric complexes with two-carbon chains between the imine and amine nitrogen atoms in that it gives a nearly axial **g** tensor. It is likely that the ferric cations in these materials have the same meridional structure as pictured in Figure 1 for FeE.

At first glance the complexes may be divided into two categories—those with rhombic **g** tensors (the first five entries in Table XII[51]), and those with essentially axial **g** tensors (the last three entries). For all complexes, the ground-state Kramers doublet, $\Gamma_1(^2T_{2g})$, is comprised almost totally of an unpaired electron in a $d_{xy}$ orbital. This finding is consistent with the negative sign that was deduced for $V_{zz}$, the principal component of the electric field gradient, from magnetic Mössbauer measurements for FeP. It is also apparent from Table XII[51] that the first excited-state low-spin Kramers doublet is at least ~2000 $cm^{-1}$ above the ground-state Kramers doublet ($\zeta$ = 460 $cm^{-1}$ for a free ferric ion).

The most notable difference between the complexes with rhombic **g** tensors such as FeP and those with axial **g** tensors such as FeE is the energy spacing of the three Kramers doublets that arises from the low-spin $^2T_{2g}$ state, as gauged by the ratio $E_2/E_3$. The first excited-state doublet is somewhat higher in energy in the axial complexes, but the second excited-state doublet is *much* higher in the rhombic complexes. Obviously neither the first nor the second excited-state doublet is thermally populated, but this difference in energy ordering of Kramers doublets might have some bearing on the spin-flipping dynamics in the solid state (vide infra).

**Comments and Conclusions**

In this section we shall address the fundamental question of *why* microcrystalline FeP is a rare example of a $N_4O_2$ ferric spin-crossover complex that flips spins rapidly compared to the $^{57}Fe$ Mössbauer time scale. The low-spin ⇌ high-spin interconversion is actually an intramolecular electron-transfer reaction involving electrons in the $t_{2g}$ and $e_g$ orbitals of a single ferric ion. The ferric complex is interconverting between the ground state, which is the lowest energy Kramers doublet ($\Gamma_1$) arising from the $^2T_{2g}$ state, and the lowest energy excited state, which is the array of three Kramers doublets known as the $^6A_{1g}$ state. If we represent the three $^6A_{1g}$ Kramers doublets as one parabolic function and the ground-state Kramers doublet $\Gamma_1$ from the $^2T_{2g}$ manifold as a second parabolic function, a simplified one-dimensional potential energy diagram can be prepared as illustrated in Figure 9. The potential energy of the complex is plotted as a function of the vibrational coordinate ($Q$) that is most active in converting the complex from one state to another. In this diagram the ground ($\Gamma_1$) and first excited state ($^6A_{1g}$) of the ferric complex interact via a second-order spin–orbit interaction, where each interacts with the components of the $^4T_{1g}$ excited state, and this leads to the avoided crossing indicated by the solid lines in the region where the two original parabolas cross. In terms of the simplified diagram of Figure 9 there are a number of parameters that are important. The nature of the vibronic ground state (lower surface with a potential energy barrier) of a given spin-crossover complex depends on the force constants for the two minima (original parabolas), the electronic coupling ($\Delta E_{res}$), the difference in zero-point energies ($\Delta E_0$), and the vibronic coupling that is proportional to the difference in metal–ligand

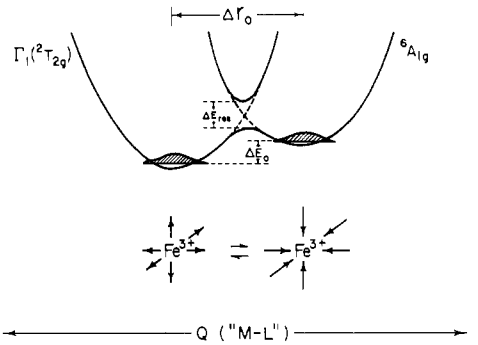


**Figure 9.** Simplified potential energy diagram for a spin-crossover complex showing the potential energy of the complex as a function of changes in the nuclear coordinate, $Q$("M–L"). The parabolic potential energy curves for the low-spin Kramers doublet ($\Gamma_1$) ground state and the high-spin $^6A_{1g}$ excited state interact via a second-order spin–orbit interaction ($\lambda(\hat{L}\cdot\hat{S})$). There is a difference in zero-point energies ($\Delta E_0$) between these two states.

distances ($\Delta r_0$) in the $\Gamma_1(^2T_{2g})$ and $^6A_{1g}$ states. In the case of the ferric spin-crossover complex, the high-spin form has a significantly longer average metal–ligand bond length ($r_{Fe-L}$ ≃ 2.07 Å for a $N_4O_2$ complex) than the low-spin form ($r_{Fe-L}$ ≃ 1.94 Å for a $N_4O_2$ complex). The ~0.13-Å greater distance in the high-spin complex results from the somewhat antibonding character of the $e_g$ orbitals, which are occupied only in the high-spin complexes.

As was pointed out in the EPR section, FeP has a rhombic **g** tensor, whereas FeE has an axial **g** tensor. In Table XII[51] it is seen that the analysis of the $g$ values for FeP places the three $^2T_{2g}$ Kramers doublets at energies of 0, 3050, and 6720 $cm^{-1}$ if the one-electron spin–orbit constant is taken as 460 $cm^{-1}$. The highest energy $^2T_{2g}$ Kramers doublet for FeE is calculated to be at 4920 $cm^{-1}$ on the basis of the $g$ values for FeE. In an (pseudo) octahedral ferric complex at the spin-crossover point the $^4T_{1g}$ excited state is expected to be ~5000–7000 $cm^{-1}$ above the barycenter of the $^2T_{2g}$ state. The rhombic nature of the FeP complex could have pushed the highest energy $^2T_{2g}$ doublet up in be~5000–7000 that it interacts more with one or more doublets from the $^4T_{1g}$ state. This would tend to increase the interaction between the $^4T_{1g}$ excited state and the ground-state $\Gamma_1(^2T_{2g})$ and therefore the interaction between the $\Gamma_1(^2T_{2g})$ and $^6A_{1g}$ states. An increase in this latter interaction would reduce the barrier height in Figure 9 and increase the spin-flipping rate. There is no direct information on the location of the $^4T_{1g}$ excited-state doublets.

How general is the above observation? Maeda et al.[39] very recently reported the EPR characteristics of the two fast $[Fe(acen)X_2]BPh_4$ spin-crossover complexes. The X = 4-methylpyridine complex does have a relatively rhombic **g** tensor; however, the rhombicity in the EPR signal for the other complex is *not* too great. However, the **g** tensor for the other fast spin-crossover complex is close to axial and not too unlike the **g** tensor observed for FeE. A solid sample of their third fast $N_4O_2$ spin-crossover complex, $[Fe(bzpa)_2]PF_6$, prepared in our laboratories gave an extremely broad EPR signal at room and liquid-nitrogen temperatures (weak intermolecular exchange interactions?). On the other hand, a frozen acetone/toluene solution gave a well-resolved EPR signal for $[Fe(bzpa)_2]PF_6$ with an axial **g** tensor ($g$ values of 2.171 and 1.970). It is clear that there is no simple relationship between $g$ values for the $\Gamma_1(^2T_{2g})$ ground state and the spin-flipping rate. There does not seem to be any clear-cut evidence for enhanced electronic interaction between the $\Gamma_1(^2T_{2g})$ and $^6A_{1g}$ states in the fast spin-flipping $N_4O_2$ complexes.

Steric factors relating to the ligand can also affect the rate of spin-state interconversion. With reference to Figure 9, if the dimensions of the complex in the $\Gamma_1(^2T_{2g})$ and $^6A_{1g}$ states are constrained to be *not* very different, this moves the minima for the two parabolas closer together and reduces the height

and thickness of the potential barrier. Wilson, Sutin, and Beattie[15-24] have commented on the influence of steric effects for solution-state species. In the case of FeP, for example, steric bulk at the aziridine donor may lengthen the shorter low-spin Fe–N(aziridine) bond but have no effect on the already longer high-spin Fe–N(aziridine) distance. Until very recently, it was just this steric hindrance associated with the aziridine donor that we held as the cause of the relatively fast spin-state interconversion rate observed for FeP. However, single-crystal X-ray structural results obtained for the 3-ethoxy-substituted form of FeP, specifically the benzene solvate $[Fe(3\text{-}OEt\text{-}SalAPA)_2]ClO_4 \cdot C_6H_6$, have shown[52] that this is *not* the explanation. The 300 K X-ray structure and preliminary 128 K X-ray structure of this complex show that there is an appreciable change in the Fe–N(aziridine) bond distance.

In summary, at this time there does *not* seem to be any obvious *intrinsic* factor that leads FeP and the three Maeda[37-39] $N_4O_2$ ferric spin-crossover complexes to interconvert in the solid state between low-spin and high-spin states faster than the $^{57}Fe$ Mössbauer time scale, compared to the slow interconversion of other $N_4O_2$ ferric complexes. It would be interesting to know whether these same $N_4O_2$ ferric complexes flip spin relatively rapidly in solution as they do in the solid state. In the next two papers in this series we will examine whether there are any effects of *inter*molecular interactions in the solid state upon the rate of spin interconversion.

**Acknowledgment.** We are grateful for support from NIH Grant HL13652. Partial funding for the Mössbauer equipment came from NSF Grant CHE-78-20727, combined with equal funding from our chemistry department and the Research Board of the University of Illinois. We thank Mark Timken for running EPR spectra of $[Fe(bzpa)_2]PF_6$. Lastly, we are indebted to Prof. C. A. Root of Bucknell University for his guidance in the development of the original synthetic method 1.

**Registry No.** FeE, 92220-29-6; CoE, 92220-31-0; FeP, 79151-63-6; APA, 1072-65-7; $[Co(SalAEA)_2]Cl$, 92220-32-1; $Fe(ClO_4)_2$, 13933-23-8; ferrous chloride, 7758-94-3; salicylaldehyde, 90-02-8.

**Supplementary Material Available:** Figure of Mössbauer spectra and listings of microanalytical data (Table I), interplanar spacings (Table II), magnetic susceptibility data (Tables III–VII), Mössbauer parameters (Tables VIII and XI), and EPR parameters (Table XII) (17 pages). Ordering information is given on any current masthead page.

---

Contribution from the School of Chemical Sciences, University of Illinois, Urbana, Illinois 61801

# Dynamics of Spin-State Interconversion and Cooperativity for Ferric Spin-Crossover Complexes in the Solid State. 2. Perturbations of the Fast Spin-Flipping $N_4O_2$ Complex $[Fe(SalAPA)_2]ClO_4$

WAYNE D. FEDERER[1] and DAVID N. HENDRICKSON*

*Received January 13, 1984*

The complex $[Fe(SalAPA)_2]ClO_4$ is a ferric spin-crossover complex that flips spin faster than the $^{57}Fe$ Mössbauer time scale. The effects on the dynamics of spin-state interconversion of various perturbations of this complex are investigated. Solvation to give $[Fe(SalAPA)_2]ClO_4 \cdot CH_2Cl_2$ dramatically affects the temperature at which there are equal amounts of high- and low-spin complexes, shifting this temperature from 295 K for the unsolvated complex to 152 K for the $CH_2Cl_2$ adduct. The $CH_2Cl_2$ adduct is still flipping spin faster than the $^{57}Fe$ Mössbauer time scale at all temperatures; however, the line widths of the two components of the one doublet at each temperature are considerably broader than the corresponding features observed for the unsolvated complex. Grinding $[Fe(SalAPA)_2]ClO_4$ with a mortar and pestle changes the Mössbauer spectra for this complex such that across a broad temperature range (~100–230 K) there are two quadrupole-split doublets present. For one hand-ground sample, the introduction of an external 30-kG field at 5 K in the Mössbauer experiment shows that the "new" doublet is associated with "residual" high-spin ferric complexes. Grinding causes broadening of the low-spin EPR resonances at all temperatures, from which it is inferred that the residual high-spin complexes are located within the same crystallites as the complexes participating in the dynamic spin-state interconversion.

## Introduction

In the preceding paper microcrystalline samples of the spin-crossover complex $[Fe(SalAPA)_2]ClO_4$, where SalAPA is the monoanionic Schiff base derived from salicylaldehyde and *N*-(3-aminopropyl)aziridine, were prepared by two different methods and were found to give appreciably different variable-temperature Mössbauer spectra. In the case of one preparative method a microcrystalline sample of $[Fe(SalAPA)_2]ClO_4$ (hereafter called FeP) is obtained directly from the reaction medium. The Mössbauer spectra for this material can be fit reasonably well to one quadrupole-split doublet at all temperatures. It is necessary to recrystallize from a dichloromethane/cyclohexane solution to obtain a microcrystalline sample from the second preparative method. There are clearly two resolved quadrupole-split doublets in each of the Mössbauer spectra at temperatures below ~233 K for this second type of microcrystalline $[Fe(SalAPA)_2]ClO_4$. This is true in spite of the fact that both samples have nearly identical analytical, infrared, and X-ray powder diffraction data. Apparently, in the first case, the FeP complexes are interconverting between low-spin and high-spin states appreciably faster than can be detected by the Mössbauer technique ($k > \sim 10^7\ s^{-1}$) and a *single* population-weighted doublet is seen. It was further suggested in the preceding paper that the microcrystals obtained from the recrystallization method are less crystalline than the microcrystals obtained from the other preparative method. The additional quadrupole doublet could then arise either from FeP complexes in the solid that are persisting in the high-spin state or from FeP complexes that are interconverting somwhat slower than the rapidly interconverting complexes. The increased concentration of defect structure (i.e., dislocations, fissures, cracks on the crystal surfaces, etc.) in the less crystalline FeP sample could be responsible for the presence of the second, "slow" FeP complex.

In this paper an effort has been made to get additional insight into the factors leading to the differences in the Mössbauer characteristics of microcrystalline FeP prepared by the two different methods. More direct evidence was also

(1) 3M Fellowship, 1979–1980. Owens-Corning Fellowship, 1980–1981. Present address: Magnetic Audio/Video Products Division, 3M, St. Paul, MN 55144.

0020-1669/84/1323-3870$01.50/0 